JJEE

Volume 12 | Number 3 | September 2026 | Pages 465-482

Jordan Journal of Electrical Engineering

ISSN (print): 2409-9600, ISSN (online): 2409-9619

Homepage: jjee.ttu.edu.jo

Analytical Approximation of Induction Motor Reactance Using Symbolic Machine-Derived Models

Ahmad Al-Subhi[1], Md Reyaz Hussan[2*], Md Shafiullah[2, 3]

[1] Electrical and Electronic Engineering Department, Yanbu Industrial College, Yanbu, Saudi Arabia
[2] IRC for Sustainable Energy Systems, King Fahd University of Petroleum & Minerals, Dhahran 31261, Saudi Arabia
[3] Control and Instrumentation Engineering Department, King Fahd University of Petroleum & Minerals, Dhahran 31261, Saudi Arabia
E-mail: mohammad.hussan@kfupm.edu.sa

Received: Nov 04, 2025 *Revised: Apr 23, 2026* *Accepted: May 11, 2026* *Available online: Aug 15, 2026*

***Abstract*—** This paper predicts the induction motor magnetizing reactance using three symbolic regression methods. TuringBot, Eureqa, and HeuristicLab have been employed in this paper to develop easy and accurate mathematical models for the reactance of single and double-cage induction motors. The reactance can be instantly evaluated using these models by knowing only a few parameters from the motor nameplate data, and without doing any field measurements. The performance of the developed models has been benchmarked with various previous methods reported in the literature. The developed models have demonstrated efficient performance with a high level of predictability for the reactance. The results show that the coefficients of determination and root mean square errors for the testing phase using TuringBot, Eureqa, and HeuristicLab are 0.997946 and 0.014544, 0.998337 and 0.013088, and 0.99622 and 0.019732, respectively.

***Keywords*—** Motor reactance; Symbolic regression; TuringBot; Eureqa; HeuristicLab.

1. INTRODUCTION

Induction motors do not require brushes, slip rings, or a commutator to function. Furthermore, the stator and rotor are not in direct contact with one another. Due to these characteristics, induction motors are long-lasting and require minimal maintenance [1]. The absence of a brush mechanism in induction motors prevents both mechanical losses from friction between the commutator and brush as well as electrical losses from the brush. Besides these advantages, squirrel-cage induction motors also offer good speed regulation, which responds well to changes in load. Due to these numerous benefits, induction motors are widely used and preferred in industrial applications. Nowadays, induction motors have largely replaced DC motors in applications due to the rapid advancements in semiconductor devices and control technologies [2]. Examples of applications include electric vehicles, the gas industry, transportation, and oil extraction mills. Compared to other motors, induction motors have several advantages, including reliability, ease of manufacturing, durability, low maintenance, and, most importantly, their cost [3].

Advances in semiconductor technology, modeling, and control have increased the attractiveness of induction motors for DC motor-like speed control tasks [4]. Consequently, induction motors are widely deployed in industry and are increasingly used in electric mobility

* Corresponding author

DOI: https://doi.org/10.5455/jjee.204-1762238377

applications. The research community is interested in developing techniques to characterize induction motors better and enhance their torque performance [5]. Modeling of an induction motor is an essential aspect for studying its behavior and characteristics. The equivalent circuit model of the induction motor comprises various parameters that must be evaluated. It is thus vital to precisely identify them in order to examine and assess the performance of the induction motor. The induction motor parameters are typically estimated using three tests: the DC test, the no-load test, and the locked-rotor test. A challenge in this regard is the need for an experimental testbed and measuring instruments. This is an inefficient approach to parameter estimation, particularly when the estimation time is a critical factor. Thus, exploring methods and algorithms that can rapidly estimate induction motor parameters using only nameplate data is crucial [6].

Several techniques have been proposed to estimate induction motor parameters [7-14]. The methods may vary in several ways, including execution time, complexity, algorithm stages, and accuracy. In [7], parameters are calculated either during changes in the system (transient state) or when the system is stable (steady state) by using a curve-fitting technique. A new approach for determining the parameters of squirrel-cage induction motors was described in [15]. This method utilizes electrical power and mechanical speed measurements obtained during a free acceleration test to estimate the parameters of the double-cage model. Additionally, the vortex search algorithm is employed to calculate the parameters and torques of an induction motor in [5].

An improved sensorless vector control of an induction motor based on an enhanced adaptive Luenberger observer is presented in [3]. Using measured stator currents, stator voltages, and predicted rotor fluxes, the suggested observer estimates motor characteristics and speed. A Takagi-Sugeno neuro-fuzzy inference system for controlling stator reactive power and direct torque in a doubly fed induction motor (DFIM) is proposed in [16]. A control system comprising a first-order Takagi-Sugeno fuzzy logic controller and a neuro-fuzzy inference system determines the control variables (d-axis and q-axis rotor voltages). In [17], a fuzzy logic-based improved direct torque control technique is presented, where torque and flux hysteresis controllers are replaced with fuzzy controllers, and a fuzzy stator resistance estimator is also utilized. To enhance the performance of induction motor drives, [18] combines parameter-adaptive indirect vector control (PA-IVC) with an optimized fractional-order proportional-integral (FOPI) controller and a randomized evolving Takagi-Sugeno (ReTSK)-adaptive neuro-fuzzy (ANF) estimation algorithm. A nonlinear observer design method for induction motors based on the Takagi-Sugeno (T-S) fuzzy controller is presented in [19].

Machine learning (ML) has emerged as a promising approach for modeling complex nonlinear systems using experimental data. In the context of induction motor parameter estimation, ML techniques enable accurate identification of parameters without relying on detailed analytical models. These methods leverage data-driven learning to capture system dynamics under varying operating conditions [20]. Table 1 summarizes the machine learning techniques applied to induction motor parameter estimation during the period 2015–2025.

The approach in [2] presents an online estimation of stator and rotor resistance in induction motors for speed sensorless vector-controlled drives using feedforward artificial neural networks with advanced adaptive learning rates. In order to predict the induction motor parameters in single-cage and double-cage models, Ref. [6] presents two innovative methods based on ANN and adaptive neuro-fuzzy inference systems (ANFIS). This was accomplished by testing 20 induction motors with varying power ratings, using data provided by the manufacturer. In [21], motor magnetizing reactance (X_m) for both single-cage and double-cage models is accurately predicted using an ANN. The relative efficacy of the suggested approaches was compared. Feed Forward Neural Networks (FFNN) were used in [1] to estimate the electrical characteristics of squirrel-cage induction motors for both single-cage and double-cage models. A new, unmemorized Elman Neural Network (ENN) structure was also proposed, in addition to the FFNN. Using manufacturer-provided data, Ref. [22] presents a dependable and versatile approach that employs an ANN to estimate the parameters of the equivalent electrical circuit of three-phase induction motors.

Table 1. Machine learning methods employed for induction motor parameters estimation.

Machine learning method	Estimated parameters	Reference	Year
Artificial Neural Network	stator and rotor resistance	[2]	2024
Artificial Neural Network, Adaptive Neuro-Fuzzy Inference Systems	stator and rotor resistance, motor reactance	[6]	2016
Artificial Neural Network	motor reactance	[21]	2024
Feed Forward Neural Network, Elman Neural Network	stator and rotor resistance, motor reactance	[1]	2020
Artificial Neural Network	stator and rotor resistance, motor reactance	[22]	2024

Machine learning methods have not been extensively utilized in the literature, particularly symbolic regression methods that construct mathematical models based on the parameters under study using nameplate data. The study presents a new approach for estimating the reactance of both double-cage and single-cage induction motors. Symbolic regression methods, including TuringBot, Eureqa, and HeuristicLab, have been used to create accurate mathematical models. Fig. 1 presents the overall study concept, clarifying the underlying objective and the resulting inferences.

Some of the merits of the proposed mathematical models are as follows:

- They are dependent on several parameters, including maximum torque to total load torque ratio, initial current to total load current ratio, full load power factor, and full load efficiency.
- Secondly, the same mathematical models apply to both single-cage and double-cage induction motors.
- Across extensive comparisons, the symbolic-regression family consistently delivered the highest predictive accuracy.
- Because the models are interpretable and inexpensive to compute, they can be embedded in design environments, digital twin processes, or on-site engineering calculators to produce fast, explainable X_m estimates.

The paper is structured as follows. Section 2 presents the equivalent circuit models of single-cage and double-cage squirrel-cage induction motors. The data set under study is discussed in Section 3. The three symbolic regression methods used to obtain the required mathematical models for estimating the motor reactance are discussed in Section 4. In Section 5, numerical results and a comparative analysis of the results obtained are presented. Section 6 concludes the paper.

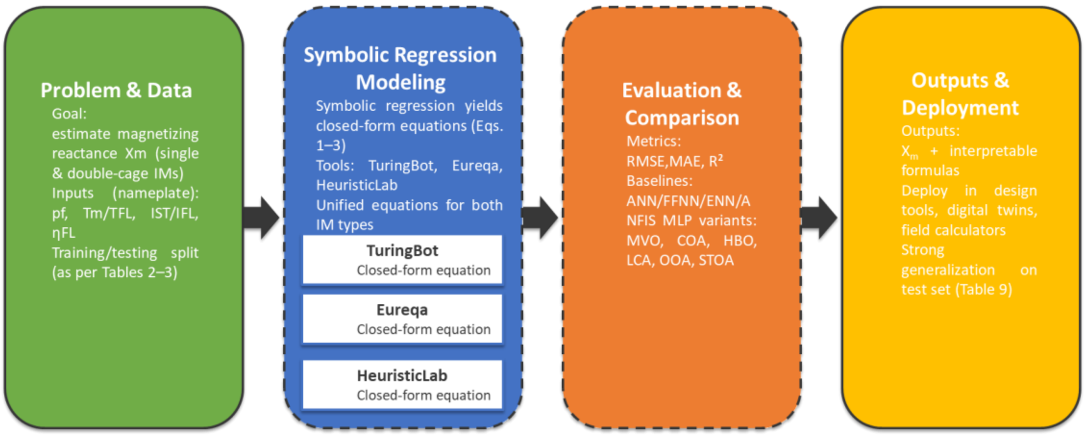

Fig. 1. Architecture of the proposed work.

2. EQUIVALENT CIRCUITS OF SQUIRREL CAGE INDUCTION MOTOR

Fig. 2 depicts squirrel-cage induction motors, depending on whether the rotor has a single-cage or double-cage structure [23]. The rotor of a squirrel-cage induction motor is constructed by stacking laminated steel sheets, which are accurately shaped and pressed into a solid core. Conductive bars, typically aluminum or copper, are embedded into longitudinal slots on the rotor surface using casting or similar manufacturing processes to form the cage structure. This configuration is known as a squirrel-cage rotor [24].

2.1. Single Cage

In several previous studies, induction motors have been represented using the classical single-cage equivalent circuit for performance analysis and parameter estimation [1, 6, 25-27]. The parameters of the single-cage equivalent circuit of an induction motor are typically determined through different tests, and these include the DC test, no-load test, and blocked-rotor test [28]. Single-cage modeling is commonly applied to wound rotor induction motors. The corresponding equivalent circuit representation of the double-cage induction motor is illustrated in Fig. 2(a), where, V_s represents the stator voltage, I_s the stator current, I_r the rotor current, s slip, R_s the stator resistance, R_r rotor resistance referred to the stator, X_{sd} stator leakage reactance, X_{rd} rotor leakage reactance referred to the stator, and X_m magnetizing reactance.

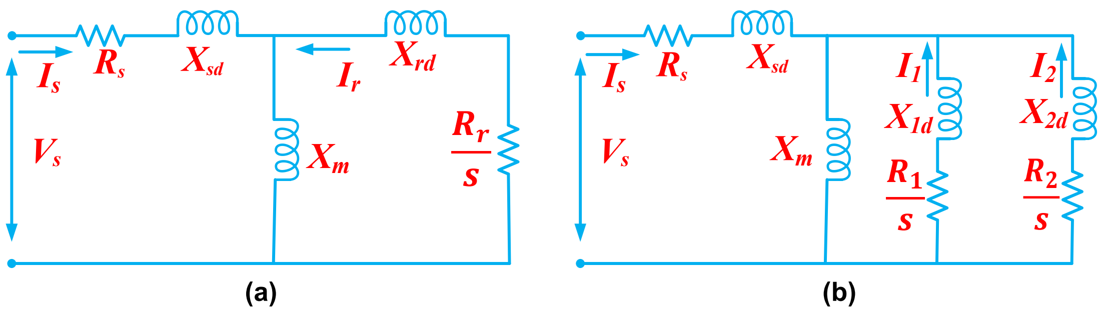

Fig. 2. Steady-state model of a) single-cage motor; and b) double-cage motor.

2.2. Double Cage

For more accurate dynamic analysis of squirrel-cage induction motors, the double-cage model is preferred. Unlike the single-cage model, which includes five distinct parameters, the double-cage model incorporates seven parameters, providing a more detailed representation of the motor's behavior. The corresponding equivalent circuit representation of the single-cage induction motor is illustrated in Fig. 2(b), having seven parameters, R_s, R_1, R_2, X_{sd}, X_{1d}, X_{2d}, and X_m. Among the parameters of the double-cage model, X_{1d} and R_1 represent the reactance and resistance of the inner cage, respectively. At the same time, X_{2d} and R_2 correspond to the reactance and resistance of the outer cage.

3. DATASET UNDER STUDY

The data used in this study were taken from [6]. Authors in [21] calculated the experimental data given in Table 2 using a numerical method presented in [9, 29]. The input parameters of the induction motor are: rated power (P), full-load power factor ($Cos(\varphi_{FL})$), the ratio of maximum torque to full-load torque (T_m/T_{FL}), the ratio of starting torque to full-load torque (T_{st}/T_{FL}), the ratio of starting current to full-load current (I_{ST}/I_{FL}), angular speed (ω_{FL}), and full-load efficiency (η_{FL}). Reactance (X_m) is the output variable of the induction motor. To be consistent with previous works [1, 6, 21], the same training and testing datasets have been adopted, as shown in Tables 2 and 3.

Table 2. Input and output data values for the Induction motor used for training.

Input								Output
P [kW]	$cos(\varphi_{FL})$	T_m/T_{FL}	T_{st}/T_{FL}	I_{ST}/I_{FL}	ω_{FL} [rpm]	η_{FL}	Cage Number	Reactance X_m [Ω]
8	0.74	2.5	2.1	4.6	960	0.86	1	1.056
11	0.9	3.1	2.2	7	2945	0.91	1	2.5856
15	0.92	2.9	2.2	6.6	2910	0.904	1	3.1806
19	0.84	3.2	2.7	6.9	1460	.905	1	1.6808
30	0.88	2.7	2.3	6	2940	0.91	1	2.3497
37	0.86	3.1	2.5	7	1475	0.929	1	1.9975
45	0.81	2.3	2.1	6	740	0.92	1	1.6728
75	0.86	2.4	2.1	6.3	1482	0.947	1	2.3228
90	0.86	2.7	2.2	6.8	1480	0.94	1	2.1573
110	0.86	3.0	2.0	7.6	2982	0.955	1	2.1294
160	0.86	2.7	2.4	7	1487	0.96	1	2.2378
200	0.87	2.7	2.7	7	1488	0.962	1	2.4082
250	0.8	3	2.2	7.3	991	0.91	1	1.4423
355	0.87	2.7	2.2	6.8	1486	0.967	1	2.4236
400	0.82	2.6	2.1	6.5	742	0.962	1	1.7943
500	0.87	2.7	2.3	6.5	992	0.966	1	2.3801
8	0.74	2.5	2.1	4.6	960	0.86	2	1.0415
11	0.9	3.1	2.2	7	2945	0.91	2	2.5947
15	0.92	2.9	2.2	6.6	2910	0.904	2	3.0787
19	0.84	3.2	2.7	6.9	1460	0.905	2	1.6559
30	0.88	2.7	2.3	6	2940	0.91	2	2.3576
37	0.86	3.1	2.5	7	1475	0.929	2	2.0088
45	0.81	2.3	2.4	6	740	0.92	2	1.7001
75	0.86	2.4	2.1	6.3	1482	0.947	2	2.3514
90	0.86	2.7	2.2	6.8	1480	0.94	2	2.1727
110	0.86	3.0	2.0	7.6	2982	0.955	2	2.1472
160	0.86	2.7	2.4	7.0	1487	0.96	2	2.261
200	0.87	2.7	2.7	7.0	1488	0.962	2	2.4351
250	0.8	3.0	2.2	7.3	991	0.91	2	1.4611
355	0.87	2.7	2.2	6.8	1486	0.967	2	2.442
400	0.82	2.6	2.1	6.5	742	0.962	2	1.8144
500	0.87	2.7	2.3	6.5	992	0.966	2	2.4021

Table 3. Input and output data values for the Induction motor used for testing.

Input								Output
P [kW]	$cos(\varphi_{FL})$	T_m/T_{FL}	T_{st}/T_{FL}	I_{ST}/I_{FL}	ω_{FL} [rpm]	η_{FL}	Cage Number	Reactance X_m [Ω]
22	0.77	2.9	2.8	5.5	975	0.908	1	1.2526
55	0.82	2.4	2.2	6	738	0.931	1	1.7594
132	0.86	3.0	2.7	7.2	1486	0.955	1	2.1209
315	0.84	3.0	2.0	7.3	991	0.962	1	1.9026
22	0.77	2.9	2.8	5.5	975	0.908	2	1.2665
55	0.82	2.4	2.2	6	738	0.931	2	1.7804
132	0.86	3.0	2.7	7.2	1486	0.955	2	2.1405
315	0.84	3	2	7.3	991	0.962	2	1.9158

It should be noted that the dataset used in this study is limited in size and is based on previously reported data. Although the adopted training and testing sets enable direct comparison with earlier studies, they may not fully capture the diversity of induction motor ratings, manufacturers, rotor designs, and operating conditions encountered in practice. Therefore, the reported predictive performance should be interpreted within the scope of the available dataset, and further validation on larger and more diverse datasets is required to confirm the generalization capability of the proposed models.

4. METHODOLOGY

To find the model that fits a given dataset, symbolic regression, a potent type of regression analysis, searches the space of mathematical expressions. Symbolic regression can extract the underlying equations or variable relationships directly from the data, in contrast to traditional regression techniques that depend on predefined functional forms [30]. Symbolic regression provides "seen" and "accessible" mathematical models, whereas ANN and other machine learning methods are often hidden and inaccessible. Symbolic regression methods improve knowledge of the structural features of complex processes and system dynamics. It is beneficial in fields where the interactions between variables are complex and poorly understood due to its capacity to infer relationships without making any assumptions beforehand. New correlations, such as astrophysical scaling laws and analytical formulations in exoplanet transit spectroscopy, have been discovered using symbolic regression. These methods rely on optimization techniques, such as genetic algorithms and simulated annealing, to construct instruction trees, where nodes represent constants, data attributes, or mathematical operations [31]. The three methods used here are machine learning-based symbolic regression tools that provide mathematical models. Fig. 3 shows the basic block diagram of the symbolic regression models.

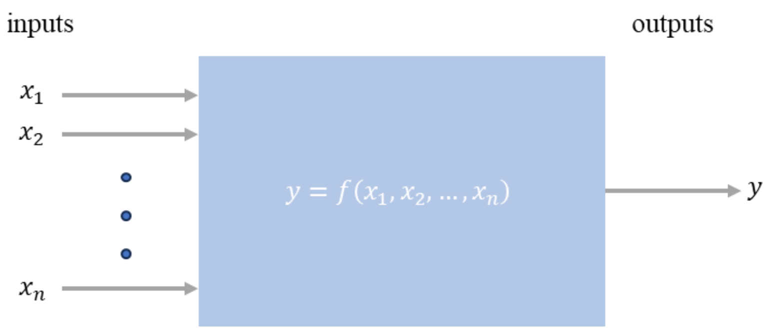

Fig. 3. Basic block diagram of TuringBot, Eureqa, and HeuristicLab.

4.1. TuringBot

TuringBot is a desktop application that utilizes symbolic regression to derive mathematical models from a given dataset. It is used to identify simple mathematical expressions that best represent the relationship between measured input and output data. Instead of relying on black-box techniques, it gives interpretable equations that explain the relationships between inputs and outputs. It employs optimization methods, such as genetic algorithms and simulated annealing, which enable it to construct expression trees comprising constants, variables, and mathematical operations. This approach makes TuringBot especially useful in research areas where understanding the underlying system behavior is just as crucial as making accurate predictions [32]. The input parameters, $x_1, x_2, \dots, x_n$ and the corresponding output parameter y are measured experimentally or obtained by simulations. These data sets are then used by the TuringBot software to formulate mathematical models. The user has the option to choose the best model that fits their requirements [31].

4.2. Eureqa

Eureqa is widely regarded as the gold standard in symbolic regression. It is based on the genetic programming (GP) framework introduced by Schmidt and Lipson [33]. It leverages a genetic algorithm-based symbolic regression technique to explore the hidden mathematical relationships from raw data. Unlike traditional regression methods, it requires no predefined functional form, allowing for minimal prior assumptions. Although the number of expression evaluations is neither tunable nor visible to the user, the software offers multiple runtime configurations. Eureqa identifies the best-fit expression by minimizing mean squared error (MSE) and also provides a Pareto front of candidate solutions based on a proprietary complexity metric [34]. Despite its strong search capability, Eureqa, like other evolutionary algorithms, can sometimes converge to a local optimum rather than the global optimum because its genetic search process is stochastic [35, 36].

4.3. HeuristicLab

HeuristicLab is an extensible optimization software system developed in the early 2000s, built around a robust metaheuristic software framework. Version 3.3 that was released in 2010 offers support for a wide variety of machine learning algorithms, such as neural networks, support vector machines, and random forests, as well as metaheuristic optimization techniques like genetic programming, evolutionary computation, particle swarm optimization, and simulated annealing. It employs a meta-model architecture that enables the flexible representation and composition of arbitrary optimization algorithms. Its graphical user interface can be used to define and manipulate metaheuristic designs intuitively. Additional capabilities include access to a library of benchmark problems and interactive visualization tools for analyzing results [37].

In practical applications, such as the training of energy flow controllers, HeuristicLab demonstrates strong interoperability, particularly through its integration with MATLAB Simulink [38]. During training, HeuristicLab initiates a MATLAB script that converts a defined Simulink model into C-code, augments it with necessary functionality, and compiles it into a dynamic-link library (DLL). This DLL is then further used by HeuristicLab to evaluate candidate solutions. Specifically, symbolic regression trees from each solution candidate are passed to the DLL along with input data, and the model is simulated to assess performance.

In the search of each symbolic regression tool, there were several candidate expressions. The final model selected was based on a tradeoff between predictive accuracy and mathematical simplicity. Specifically, candidate models with smaller RMSE (root mean square error) and larger R^2 (coefficient of determination) were favored, as long as their analytical form could be expressed fairly compactly and interpreted. This criterion was adopted to prevent unnecessarily complicated formulas and to enhance the usability of the developed models.

In order to enhance reproducibility, the general workflow that is followed in this study can be summarized as follows. To begin with, the data was divided into training and testing data sets based on the same split that had been used in other related research. Each of the symbolic regression tools (TuringBot, Eureqa, and HeuristicLab) was then given the input variables to produce candidate analytical expressions to estimate X_m. Each tool tried various candidate models, and the best model was ultimately picked based on a tradeoff of predictive accuracy and simplicity of expression. Finally, RMSE, MAE, and R^2 were used to assess the models on the testing set and compare them to other methods that had been reported previously.

5. RESULTS AND ANALYSIS

The performance of the three symbolic regression models for estimating the reactance of single-cage and double-cage induction motors will be evaluated in this section. TuringBot, HeuristicLab, and Eureqa are benchmarked against feedforward neural network (FFNN), ensemble neural network (ENN), artificial neural network (ANN), and adaptive neuro-fuzzy inference system (ANFIS) models reported in [1]. Their predictive accuracy was assessed using three statistical indicators: root mean squared error (RMSE), mean absolute error (MAE), and coefficient of determination (R^2). They are also compared with the other six approaches for the target estimation task. These are metaheuristic-optimized multilayer perceptrons, namely multi-verse optimization- multilayer perceptron (MVO-MLP), cuckoo optimization algorithm-MLP (COA-MLP), heap-based optimization -MLP (HBO-MLP), leagues championship algorithm -MLP (LCA-MLP), osprey optimization algorithm-MLP (OOA-MLP), sooty tern optimization algorithm-MLP (STOA-MLP), suggested in [21].

5.1. Developed Models

The motor reactance (X_m) for single-cage and double-cage induction motors was predicted using three mathematical models obtained by applying three symbolic regression methods: TuringBot, Eureqa, and HeuristicLab. One of the merits of these models is that the same mathematical model can estimate the motor reactance for both single-cage and double-cage induction motors. Equations (1), (2), and (3) represent the mathematical models obtained for estimating motor reactance using symbolic regression methods, TuringBot, Eureqa, and HeuristicLab, respectively. Among the candidate symbolic regression expressions, the final models reported in this paper were selected based on the best tradeoff between accuracy and simplicity. From a computational perspective, the proposed symbolic-regression models are also attractive because they are expressed in closed form and can be evaluated using only a limited number of algebraic operations. Once derived, their implementation requires only direct substitution of the input variables into the analytical expressions, which makes them lightweight and suitable for fast engineering calculations. In contrast, ANN, FFNN, ENN, and ANFIS based approaches generally require matrix operations, nonlinear activation evaluations, and more complex model structures during inference. Therefore, beyond interpretability, the proposed symbolic-regression models also offer a lower implementation burden for practical X_m estimation.

$$X_m = \left(0.0599465 + Cos(\varphi FL) - \left(\frac{-0.22252}{\left(\frac{5.49351}{{I_{ST}}/{I_{FL}}} \right) - \eta_{FL} + {T_m}/{T_{FL}}} \right) \right)^{13.3286} + \left(\frac{-0.529914 + \eta_{FL}}{0.376374} \right) \quad (1)$$

$$X_m = 3.31092 * \eta_{FL} + 1.07859 * {T_m}/{T_{FL}} + \frac{6.46553}{Cos(\varphi FL)} + 0.04996 * {I_{ST}}/{I_{FL}} * \eta + 14.04906 * Cos(\varphi FL) * (0.82206 * Cos(\varphi FL)^2)^{{T_m}/{T_{FL}}} - 14.84853 \quad (2)$$

$$X_m = 1.5586 * \eta_{FL} + 0.20907 * Cos(\varphi FL)^2 - 0.7378 - \frac{1.4218 * {I_{ST}}/{I_{FL}} * \eta_{FL} * Cos(\varphi FL)^4}{0.66643 * {T_m}/{T_{FL}} * \left(\frac{1}{-0.23063 Cos(\varphi FL)} + 4.0703 \right) \left(0.21752 * {I_{ST}}/{I_{FL}} + 0.70289 \right)} \quad (3)$$

where $Cos(\varphi_{FL})$ represents full-load power factor, ${T_m}/{T_{FL}}$ the ratio of maximum to full-load torque, ${I_{ST}}/{I_{FL}}$ the ratio of starting to full-load current, and η_{FL} the full-load efficiency.

5.2. Comparative Analysis

The symbolic-regression models, TuringBot, HeuristicLab, and Eureqa, are compared with Feedforward Neural Network (FFNN), Ensemble Neural Network (ENN), Artificial Neural Network (ANN), and Adaptive Neuro-Fuzzy Inference System (ANFIS) models reported in [1], [40]. Secondly, metaheuristic-optimized multilayer perceptrons (MVO-MLP, COA-MLP, HBO-MLP, LCA-MLP, OOA-MLP, STOA-MLP), as suggested in [21], are also considered for comparative analysis.

5.2.1. Model assessments and comparisons

a) Single cage: testing

The data set used for testing here is new and was not involved in the training process; it is the same testing data used in previous works. Table 4 and Table 5 present the experimental and predicted values, along with the percentage error, for the single-cage induction motor using different methods reported in [1, 39] and the proposed symbolic regression models, respectively. For the single-cage induction motor dataset, the TuringBot model demonstrated the best overall performance, with an RMSE of 0.0078, an MAE of 0.0063, and an R^2 of 0.9994, indicating a near-perfect fit to the experimental data. This was closely followed by

HeuristicLab (RMSE = 0.0101, R^2 = 0.9990) and Eureqa (RMSE = 0.0167, R^2 = 0.9973). Neural-based approaches such as FFNN and ENN also produced acceptable predictions, with R^2 values of 0.9938 and 0.9762, respectively. However, ANFIS and ANN performed less favorably, with ANN showing the weakest accuracy (RMSE = 0.1018, MAE = 0.0848, R^2 = 0.8984). The results demonstrate that symbolic regression-based tools (TuringBot, HeuristicLab, Eureqa) provided superior generalization for single-cage induction motor reactance estimation compared to purely neural approaches, likely due to their ability to capture explicit analytical structures in the data. The experimental and predicted values for the single-cage induction motor, obtained using different methods, are graphically shown in Fig. 4.

Table 4. Experimental and predicted values for different methods reported in [1] for a single cage induction motor.

exp	ANFIS	error [%]	ANN	error [%]	FFNN	error [%]	ENN	error [%]
1.9026	1.9252	1.18785	2.0491	7.69999	1.9179	0.80416	1.9255	1.20362
2.1209	2.1414	0.96657	2.1274	0.30647	2.1322	0.53279	2.1998	3.72012
1.7594	1.8643	5.96226	1.7028	3.21701	1.764	0.26145	1.7639	0.25577
1.2526	1.2385	1.12566	1.1232	10.3305	1.2991	3.71228	1.3068	4.327

Table 5. Experimental and predicted values for the proposed symbolic regression models for a single cage induction motor.

exp	TuringBot	error [%]	Eureqa	error [%]	HeuristicLab	error [%]
1.9026	1.90872	0.32146	1.9234	1.09303	1.90351	0.04805
2.1209	2.11871	0.10342	2.12628	0.25372	2.11876	0.10084
1.7594	1.76248	0.17512	1.76321	0.2163	1.77223	0.72945
1.2526	1.26637	1.09961	1.27789	2.01867	1.23705	1.24124

b) Double cage: testing

Table 6 and Table 7 present the experimental and predicted values, along with the percentage error, for the double cage induction motor using different methods reported in [1] and the proposed symbolic regression models, respectively. In the case of double-cage induction motor estimation, only ANN (RMSE = 0.000158, MAE = 0.0001, R^2 = 0.9999997573) is better than the symbolic regression models. Although ANN produced an almost perfect fit for the double-cage test data, this result should be interpreted with caution. The double-cage samples are closely related to the training data and exhibit limited variability, which may favor interpolation by highly flexible neural models. Therefore, the near-perfect ANN accuracy does not necessarily guarantee superior generalization in broader practical settings. After ANN, the TuringBot model outperformed other approaches with an RMSE of 0.0145, MAE of 0.0117, and R^2 of 0.9980. Neural methods (FFNN and ENN) also provided high accuracy, with R^2 values ranging from 0.989 to 0.990, although with slightly higher errors compared to TuringBot. In contrast, ANFIS exhibited the weakest performance, with an RMSE of 0.0906 and an R^2 of 0.9203, indicating limited suitability for this dataset. This trend is consistent with the single-cage case, where symbolic regression tools demonstrated higher precision than fuzzy-neural systems. The performance gap was narrower for double-cage induction motors, indicating that the inherent nonlinearity of the dataset may favor neural methods more than in the single-cage scenario. A summary of the average error for testing only is given in Table 8. The experimental and predicted values for the double cage induction motor using different methods are graphically shown in Fig. 5. Fig. 6 and Fig. 7 represent the comparison of these methods with respect to RMSE, MAE, and R^2 values for single-cage and double-cage induction motors, respectively.

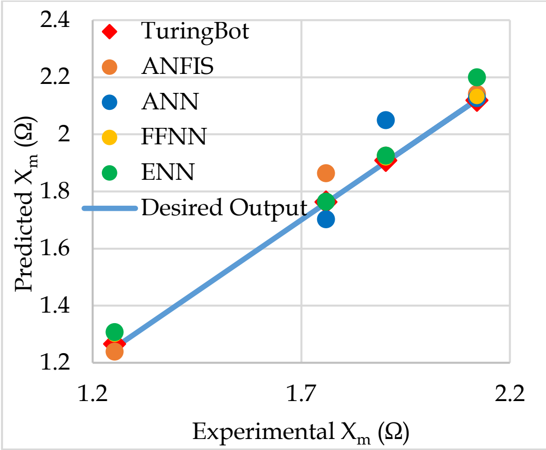

(a)

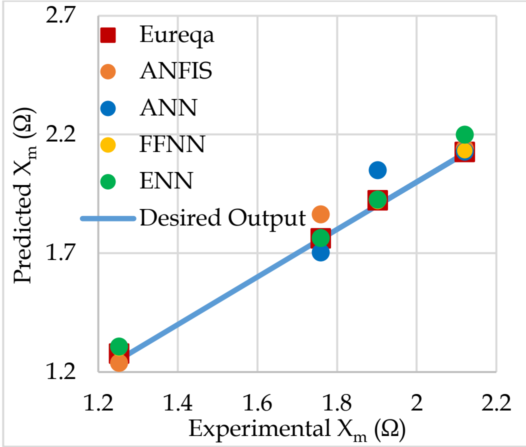

(b)

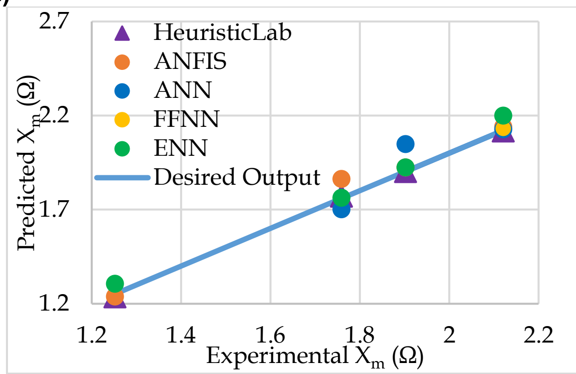

(c)

Fig. 4. Predicted versus experimental values of ANFIS, ANN, FFNN, and ENN methods for a single cage induction motor with a) TuringBot; b) Eureqa; and c) HeuristicLab.

Table 6. Experimental and predicted values for different methods reported in [1] for a double cage induction motor.

exp	ANFIS	error [%]	ANN	error [%]	FFNN	error [%]	ENN	error [%]
1.9158	1.81307	5.36225	1.9158	0	1.6733	12.6579	1.7966	6.22194
2.1405	2.26312	5.72861	2.1405	0	2.0156	5.83509	2.1439	0.15884
1.7804	1.69538	4.77533	1.7805	0.00562	1.8326	2.93193	1.7992	1.05594
1.2665	1.27111	0.36368	1.2662	0.02369	1.3721	8.33794	1.3253	4.64272

Table 7. Experimental and Predicted values for the proposed symbolic regression models for the double cage induction motor.

exp	TuringBot	error [%]	Eureqa	error [%]	HeuristicLab	error [%]
1.9158	1.90872	0.36976	1.9234	0.39649	1.90351427	0.64128
2.1405	2.11871	1.01814	2.12628	0.66428	2.11876138	1.01559
1.7804	1.76248	1.00646	1.76321	0.96576	1.77223393	0.45867
1.2665	1.26637	0.00997	1.27789	0.899	1.23705225	2.32513

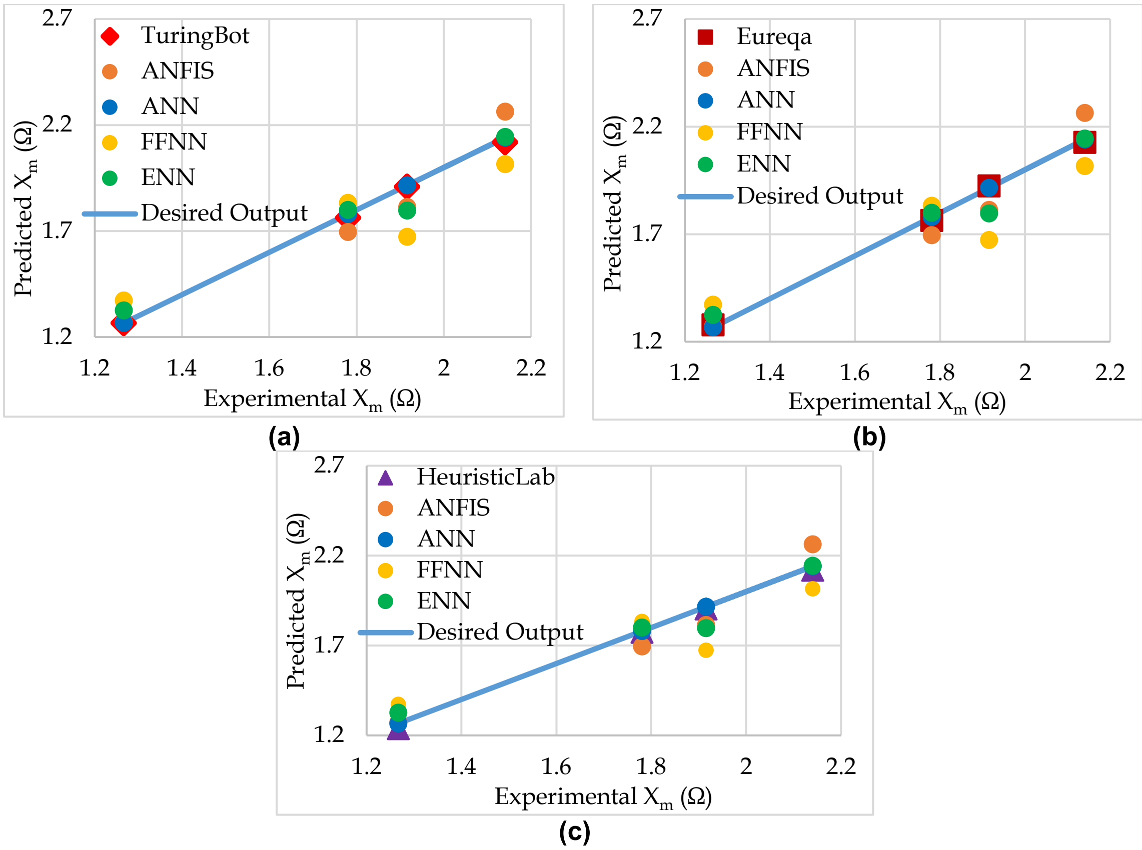

Fig. 5. Predicted v/s experimental values of ANFIS, ANN, FFNN, and ENN methods for double cage induction motor with a) TuringBot; b) Eureqa; c) HeuristicLab.

Table 8. Average error for testing only.

	Average error [%]	
Method	Single cage	Double cage
ANFIS	2.31058	4.05747
ANN	5.3885	0.00733
FFNN	1.32767	7.44071
ENN	2.37663	3.01986
TuringBot	0.4249	0.60108
Eureqa	0.89543	0.73138
HeuristicLab	0.52989	1.11017

5.2.2. Model assessments and comparisons with the six metaheuristic-optimized multilayer perceptrons reported in [21].

The proposed symbolic regression models were also compared with six metaheuristic-optimized multilayer perceptron models (MVO-MLP, COA-MLP, HBO-MLP, LCA-MLP, OOA-MLP, and STOA-MLP) reported in [21]. Their performance was evaluated using R^2 and RMSE on both the training and testing sets, as summarized in Table 9. All models achieved high accuracy on the test set ($R_{test}^2 \geq 0.97$).

However, the symbolic regression models produced the best overall test performance. Among them, Eureqa achieved the highest accuracy, with R_{test}^2 = 0.998337 and $RMSE_{test}$ = 0.013088, followed by TuringBot (R_{test}^2 = 0.997946 and $RMSE_{test}$ = 0.014544) and HeuristicLab (R_{test}^2 = 0.99622 and $RMSE_{test}$ = 0.019732). Among the MLP-based models, MVO-MLP was the best-performing baseline, with $RMSE_{test}$ = 0.020315, R^2 = 0.99598.

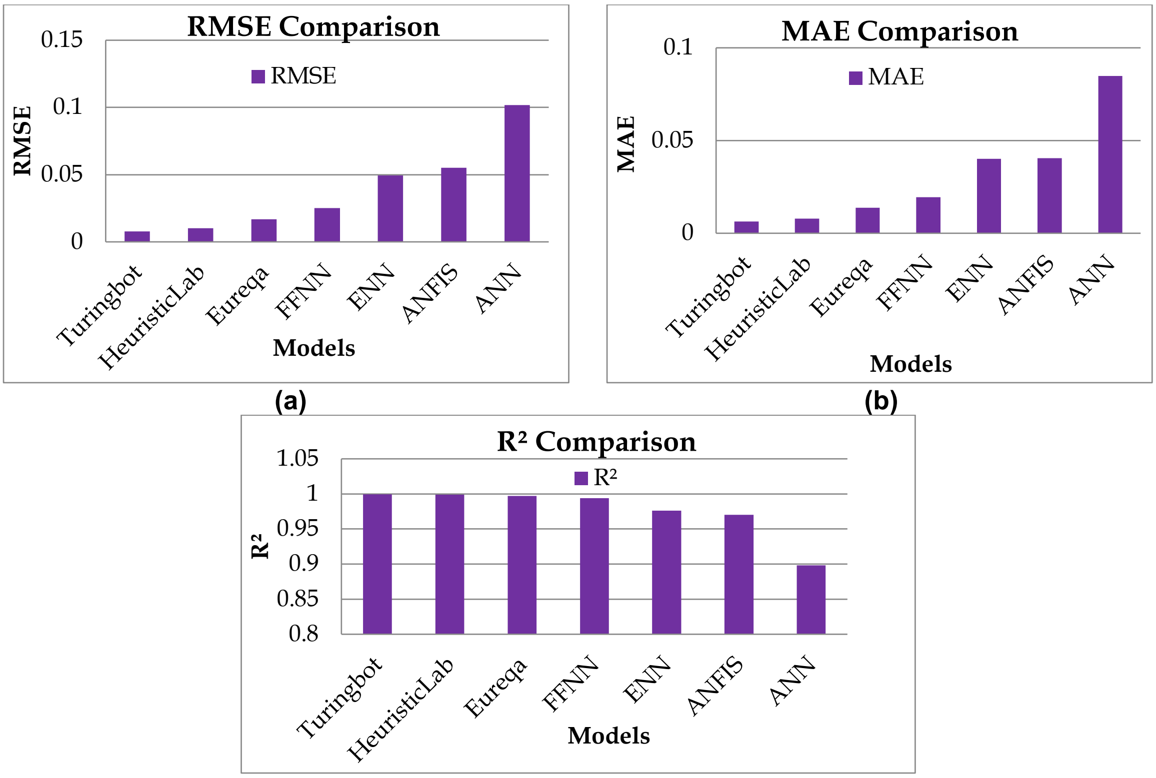

(c)

Fig. 6. Comparison of the ANFIS, ANN, FFNN, ENN, TuringBot, Eureqa, and HeuristicLab for a single cage induction motor a) RMSE; b) MAE; c) R^2.

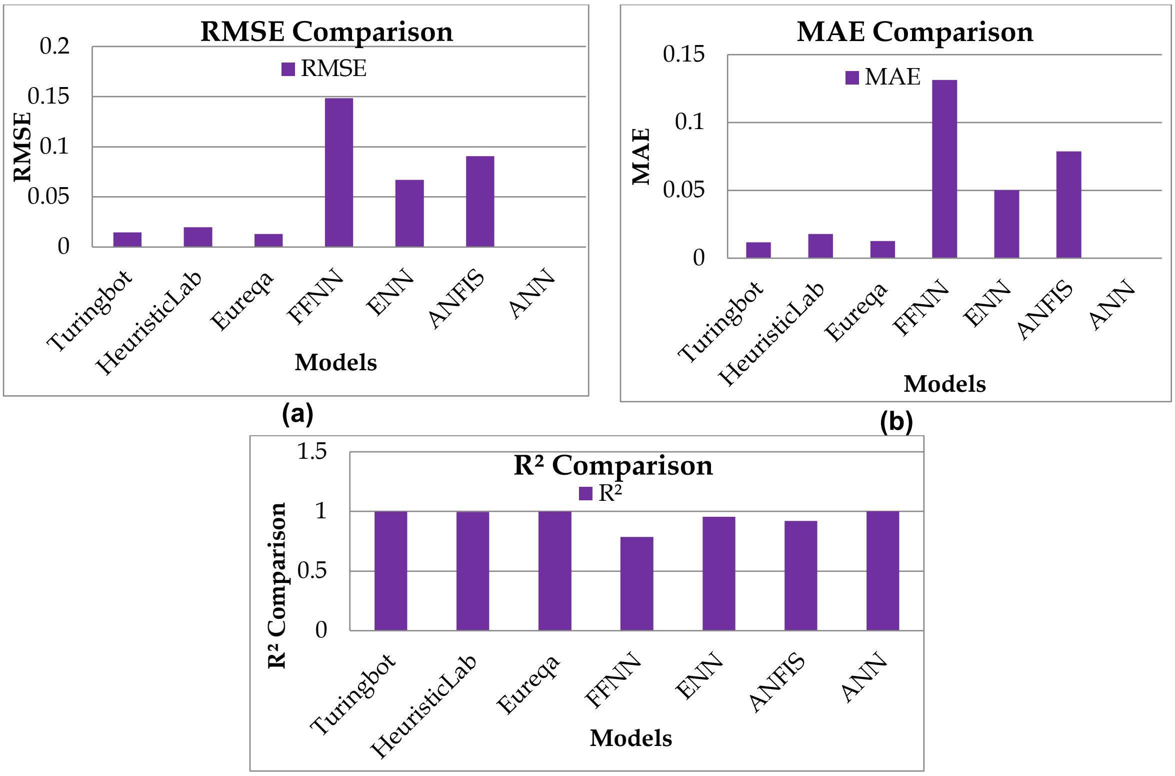

(c)

Fig. 7. Comparison of the ANFIS, ANN, FFNN, ENN, TuringBot, Eureqa, and HeuristicLab for double cage induction motor.

Fig. 8 represents the graph for comparison of the six metaheuristic-optimized multilayer perceptrons with TuringBot, Eureqa, and HeuristicLab with respect to RMSE and R^2 values. Symbolic regression models (Eureqa, TuringBot, HeuristicLab) exhibit equal or lower RMSE on the test set than on training (e.g., Eureqa: 0.032639→0.013088; TuringBot: 0.025044→0.014544; HeuristicLab: 0.023006→0.019732). This indicates no overfitting and suggests robust, parsimonious fits, consistent with symbolic regression's discovery of compact analytical forms. The stronger MLPs (e.g., MVO-MLP, STOA-MLP) generalize well but trail the symbolic regression methods by ~0.005–0.012 RMSE on the test set. OOA-MLP exhibits the highest errors on both splits, suggesting that it may have suboptimal hyperparameters or prematurely converged in its optimizer. For deployment, Eureqa and TuringBot are the most reliable choices. HeuristicLab offers a strong third option. If an MLP architecture is preferred (e.g., for compatibility or runtime constraints), MVO-MLP is the most competitive among neural baselines.

Table 9. Training and testing R^2 and RMSE values for different methods.

	Training		testing	
Method	R^2	RMSE	R^2	RMSE
MVO-MLP	0.9962	0.02081	0.99598	0.020315
COA-MLP	0.9937	0.026665	0.99358	0.025642
HBO-MLP	0.9858	0.039971	0.98561	0.038313
LCA-MLP	0.9929	0.028341	0.99252	0.027675
OOA-MLP	0.9691	0.058722	0.97008	0.055037
STOA-MLP	0.9946	0.024804	0.99395	0.024897
TuringBot	0.998647	0.025044	0.997946	0.014544
Eureqa	0.997702	0.032639	0.998337	0.013088
HeuristicLab	0.998958	0.023006	0.99622	0.019732

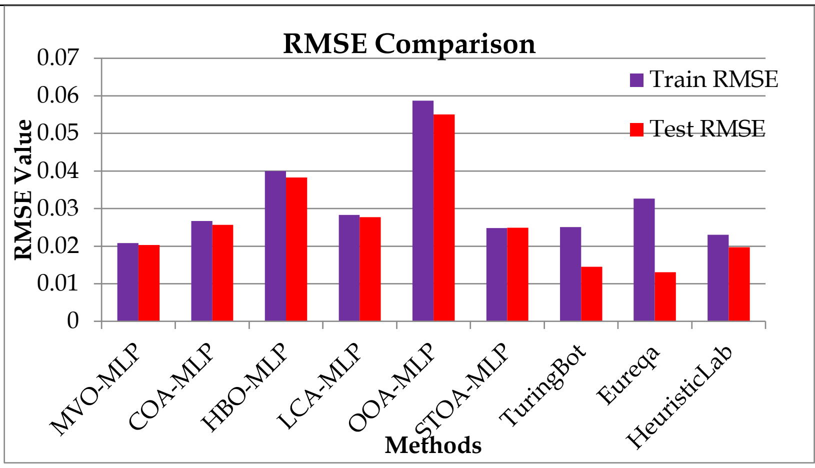

(a)

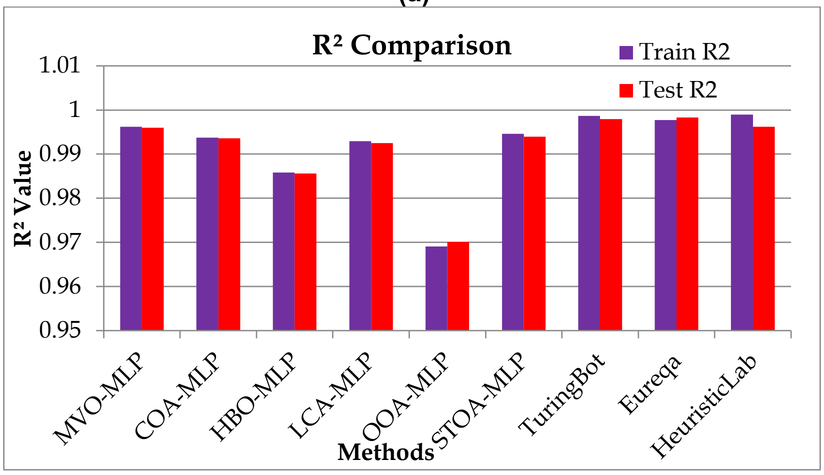

(b)

Fig. 8. Comparison of the six metaheuristic-optimized multilayer perceptrons with TuringBot, Eureqa, and HeuristicLab for a) RMSE; and b) R^2.

The comparative evaluation highlights that:

- One of the merits of the proposed symbolic regression models is that the same mathematical model can estimate the motor reactance for both single-cage and double-cage induction motors.
- Secondly, the proposed models depend on a few parameters (only four inputs, regardless of rated power, rated speed, and the ratio of starting torque to full-load torque)
- Symbolic regression approaches (TuringBot, HeuristicLab, Eureqa) consistently provided the highest predictive accuracy, with minimal errors across both induction motor types.
- Classical neural models, such as ANN, FFNN, and ENN demonstrated reasonable accuracy, although their performance was slightly inferior to that of symbolic regression tools.
- The ANFIS approach underperformed in both cases, particularly for the double-cage induction motor, suggesting that its rule-based inference mechanism may not adequately capture the nonlinear mapping in this application.

Overall, the results indicate that symbolic regression models, particularly TuringBot, are highly effective for estimating induction motor reactance from the studied data set, offering both accuracy and the advantage of interpretable analytical expressions. Neural network models remain competitive, especially for more complex double-cage induction motor dynamics, but may require additional optimization (e.g., deeper architectures, hyperparameter tuning) to match symbolic regression performance.

6. CONCLUSIONS

This paper presented three symbolic regression models, derived using TuringBot, Eureqa, and HeuristicLab, that provide compact, closed-form expressions for estimating the magnetizing reactance of both single-cage and double-cage induction motors based solely on nameplate information. All models require just four readily available inputs: full-load power factor, the ratio of maximum to full-load torque, the ratio of starting to full-load current, and full-load efficiency. The results showed that the proposed symbolic regression models achieved strong predictive accuracy on the adopted benchmark dataset. Among the compared methods, Eureqa gave the best overall test performance against the six metaheuristic-optimized MLP models, followed by TuringBot and HeuristicLab. In the comparison with classical ANN-, FFNN-, ENN-, and ANFIS-based methods, symbolic regression was generally more accurate for the single-cage case and remained highly competitive for the double-cage case. In addition to accuracy, the proposed models offer interpretable closed-form expressions and low computational cost. These findings indicate that symbolic regression provides a practical and transparent alternative for X_m estimation when laboratory testing is unavailable or inconvenient. However, the reported results should be interpreted in light of the limited dataset size. Future work should validate the proposed models on larger and more diverse datasets and extend the framework to additional induction-motor parameters.

Acknowledgement: The authors gratefully acknowledge the research support provided by the IRC for Sustainable Energy Systems at King Fahd University of Petroleum & Minerals (KFUPM) through project no. INSE2632.

REFERENCES

[1] O. Çetin, A. Dalcalı, F. Temurtaş, "A comparative study on parameters estimation of squirrel cage induction motors using neural networks with unmemorized training," *Engineering Science and Technology, an International Journal*, vol. 23, no. 5, pp. 1126–1133, 2020, doi: 10.1016/j.jestch.2020.03.011.

[2] A. Kanakabettu, R. Irvathoor, S. Saralaya, S. Jodumutt, A. Singh, "Novel advanced artificial neural network-based online stator and rotor resistance estimator for vector-controlled speed sensorless induction motor drives," *Energies*, vol. 17, no. 9, 2024, doi: 10.3390/en17092150.

[3] Z. Boulghasoul, Z. Kandoussi, A. Elbacha, A. Tajer, "fuzzy improvement on luenberger observer based induction motor parameters estimation for high performances sensorless drive," *Journal of Electrical Engineering and Technology*, vol. 15, no. 5, pp. 2179–2197, 2020, doi: 10.1007/s42835-020-00495-6.

[4] R. Boros, I. Bodnár, "Effect of SPWM inverter in combination with solar uninterruptible induction motor drive," *Energies*, vol. 16, no. 13, 2023, doi: 10.3390/en16135061.

[5] J. Montano, O. Garzón, D. Herrera-Jaramillo, O. Montoya, F. Andrade, A. Tobon, "Estimating the parameters of a three-phase induction motor using the vortex search algorithm," *Iranian Journal of Science and Technology - Transactions of Electrical Engineering*, vol. 48, no. 1, pp. 337–347, 2024, doi: 10.1007/s40998-023-00673-y.

[6] M. Jirdehi, A. Rezaei, "Parameters estimation of squirrel-cage induction motors using ANN and ANFIS," *Alexandria Engineering Journal*, vol. 55, no. 1, pp. 357–368, 2016, doi: 10.1016/j.aej.2016.01.026.

[7] H. V. Khang and A. Arkkio, "Parameter estimation for a deep-bar induction motor," *IET Electr. Power Appl.*, vol. 6, no. 2, pp. 133–142, 2012, doi: 10.1049/iet-epa.2010.0256.

[8] L. Peretti, M. Zigliotto, "Automatic procedure for induction motor parameter estimation at standstill," *IET Electric Power Applications*, vol. 6, no. 4, pp. 214–224, 2012, doi: 10.1049/iet-epa.2010.0262.

[9] J. Pedra, F. Córcoles, "Estimation of induction motor double-cage model parameters from manufacturer data," *IEEE Transactions on Energy Conversion*, vol. 19, no. 2, pp. 310–317, 2004, doi: 10.1109/TEC.2003.822314.

[10] D. Chaturvedi, M. Singh, O. Malik, "Development of integrated softcomputing approach for stator resistance estimation of three phase induction motor," *Electric Power Components and Systems*, vol. 49, no. 18–19, pp. 1489–1498, 2022, doi: 10.1080/15325008.2022.2132561.

[11] V. Sakthivel, R. Bhuvaneswari, S. Subramanian, "Bacterial foraging technique based parameter estimation of induction motor from manufacturer data," *Electric Power Components and Systems*, vol. 38, no. 6, pp. 657–674, 2010, doi: 10.1080/15325000903489660.

[12] S. Soliman, G. Chistensen, "Modeling of induction motors from standstill frequency response tests and a parameter estimation algorithm," *Electric Machines and Power Systems*, vol. 20, no. 2, pp. 123–136, 1992, doi: 10.1080/07313569208909576.

[13] M. Pudari, S. Arya, P. Ray, "Multi-parameter identification using PQ-MRAS for indirect field-oriented control IMD with optimized PI gains," *Electrical Engineering*, 2025, doi: 10.1007/s00202-025-03113-8.

[14] S. Ipek, M. Taskiran, N. Bekiroglu, E. Aycicek, "Optimal induction machine parameter estimation method with artificial neural networks," *Electrical Engineering*, vol. 106, no. 2, pp. 1959–1975, 2024, doi: 10.1007/s00202-023-02049-1.

[15] H. Kojooyan-Jafari, L. Monjo, F. Corcoles, J. Pedra, "Using the instantaneous power of a free acceleration test for squirrel-cage motor parameters estimation," *IEEE Transactions on Energy Conversion*, vol. 30, no. 3, pp. 974–982, 2015, doi: 10.1109/TEC.2015.2399697.

[16] R. Jacomini, C. Rocha, J. Altuna, J. Azcue, C. Capovilla, A. Sguarezi Filho, "Implementation of a neuro-fuzzy direct torque and reactive power control for DFIM," 40th Annual Conference of the IEEE Industrial Electronics Society, 2014, doi: 10.1109/IECON.2014.7048569.

[17] Y. Bendaha, M. Benyounes, "Fuzzy direct torque control of induction motor with sensorless speed control using parameters machine estimation," 3rd International Conference on Control, Engineering & Information Technology, 2015, doi: 10.1109/CEIT.2015.7233022.

[18] P. Mahesh, "Randomized self-structuring adaptive neuro-fuzzy based induction motor drives with optimized fopi gains," *CPSS Transactions on Power Electronics and Applications*, vol. 9, no. 4, 2024, doi: 10.24295/CPSSTPEA.2024.00026.

[19] M. Hammoudi, M. Benbouzid, N. Rizoug, A. Allag, "New state observer based on Takagi-Sugeno fuzzy controller of induction motor," 4th International Conference on Systems and Control, 2015, doi: 10.1109/ICoSC.2015.7153279.

[20] R. Thomas, R. Gupta, "A Survey on machine learning approaches and its techniques," IEEE International Students' Conference on Electrical,Electronics and Computer Sciencm, 2020, doi: 10.1109/SCEECS48394.2020.190.

[21] H. Gör, "Feasibility of six metaheuristic solutions for estimating induction motor reactance," *Mathematics*, vol. 12, no. 3, 2024, doi: 10.3390/math12030483.

[22] G. Lourenco, G. Arruda, V. Correia De Rosa, M. Castoldi, A. Goedtel, W. Souza, "Three-phase induction motor electrical parameter estimation using artificial neural networks," International Symposium on Power Electronics, Electrical Drives, Automation and Motion, 2024, doi: 10.1109/SPEEDAM61530.2024.10609175.

[23] D. Bhowmick, S. Chowdhury, "Estimation of induction motor equivalent circuit parameters and losses from transient measurement," *ISA Transactions*, vol. 157, pp. 573–590, 2025, doi: 10.1016/j.isatra.2024.12.012.

[24] A. Marfoli, M. DiNardo, M. Degano, C. Gerada, W. Jara, "Squirrel cage induction motor: a design-based comparison between aluminium and copper cages," *IEEE Open Journal of Industry Applications*, vol. 2, pp. 110–120, 2021, doi: 10.1109/OJIA.2021.3073820.

[25] L. Pereira, M. Perin, L. Pereira, J. Ruthes, F. Sousa, and E. Oliveira, "Performance estimation of three-phase induction motors from no-load startup test without speed acquisition," *ISA Transactions*, vol. 96, pp. 376–389, 2020, doi: 10.1016/j.isatra.2019.05.028.

[26] P. Aree, "Analytical approach to determine speed-torque curve of induction motor from manufacturer data," *Procedia Computer Science*, vol. 86, pp. 293–296, 2016, doi: 10.1016/j.procs.2016.05.076.

[27] J. Pedra, L. Sainz, F. Córcoles, "Harmonic modeling of induction motors," *Electric Power Systems Research*, vol. 76, no. 11, pp. 936–944, 2006, doi: 10.1016/j.epsr.2005.10.015.

[28] A. Amadou Adamou, C. Alaoui, "Energy efficiency model-based Digital shadow for Induction motors: Towards the implementation of a Digital Twin," *Engineering Science and Technology, an International Journal*, vol. 44, 2023, doi: 10.1016/j.jestch.2023.101469.

[29] L. Monjo, H. Kojooyan-Jafari, F. Corcoles, J. Pedra, "Squirrel-cage induction motor parameter estimation using a variable frequency test," *IEEE Transactions on Energy Conversion*, vol. 30, no. 2, pp. 550–557, 2015, doi: 10.1109/TEC.2014.2362964.

[30] P. Moscato, A. Ciezak, "A New approximation for the perimeter of an ellipse," *Algorithms*, vol. 17, no. 10, 2024, doi: 10.3390/a17100464.

[31] A. Carvalho, D. Oliveira, A. Krone-Martins, A. Silva, "Symbolic regression applied to cosmology: an approximate expression for the density perturbation variance," 19th International Conference on e-Science, e-Science 2023, 2023. doi: 10.1109/e-Science58273.2023.10254889.

[32] A. Al-Subhi, "Dynamic economic load dispatch using linear programming and mathematical-based models," *Mathematical Modelling of Engineering Problems*, vol. 9, no. 3, pp. 606–614, 2022, doi: 10.18280/mmep.090307.

[33] M. Schmidt, H. Lipson, “Distilling free-form natural laws from experimental data,” *Science*, vol. 324, no. 5923, pp. 81–85, 2009, doi: 10.1126/science.1165893.

[34] B. Petersen, M. Landajuela, T. Mundhenk, C. Santiago, S. Kim, J. Kim, “Deep symbolic regression: Recovering mathematical expressions from data via risk-seeking policy gradients,” 2021, http://arxiv.org/abs/1912.04871.

[35] A. Baczynska, W. Niewiadomski, ʹʹ The impact of the phase-shifting transformers on the power flow in the transmission gridʹʹ, International Conference on the European Energy Market, 2018, doi: 10.1109/EEM.2018.8469924.

[36] W. La Cava et al., “Contemporary symbolic regression methods and their relative performance HHS public access,” 2021, https://github.com/cavalab/srbench.

[37] S. Wagner, M. Affenzeller, “HeuristicLab: a generic and extensible optimization environment,” Adaptive and Natural Computing Algorithms, 2005, doi: 10.1007/3-211-27389-1_130.

[38] K. Kefer, M. Affenzeller, S. Winkler, “Adaptive operators for genetic programming to identify optimal energy flow controllers,” Procedia Computer Science, Elsevier, 2025, doi: 10.1016/j.procs.2025.01.261.

[39] H. Feng, X. Cui, J. Si, C. Gao, C. Gan, “Equivalent circuit model of novel solid rotor induction motor with toroidal winding,” *Journal of Magnetics*, vol. 24, no. 4, pp. 568–576, 2019, doi: 10.4283/JMAG.2019.24.4.568.